INFECTIOUS DISEASE

A small-molecule antivirulence agent for treating *Clostridium difficile* infection

Kristina Oresic Bender,[1]* Megan Garland,[1]* Jessica A. Ferreyra,[2] Andrew J. Hryckowian,[2] Matthew A. Child,[1] Aaron W. Puri,[1†] David E. Solow-Cordero,[3] Steven K. Higginbottom,[2] Ehud Segal,[1] Niaz Banaei,[1,4] Aimee Shen,[5] Justin L. Sonnenburg,[2] Matthew Bogyo[1,2‡]

Clostridium difficile **infection (CDI) is a worldwide health threat that is typically triggered by the use of broad-spectrum antibiotics, which disrupt the natural gut microbiota and allow this Gram-positive anaerobic pathogen to thrive. The increased incidence and severity of disease coupled with decreased response, high recurrence rates, and emergence of multiple antibiotic-resistant strains have created an urgent need for new therapies. We describe pharmacological targeting of the cysteine protease domain (CPD) within the *C. difficile* major virulence factor toxin B (TcdB). Through a targeted screen with an activity-based probe for this protease domain, we identified a number of potent CPD inhibitors, including one bioactive compound, ebselen, which is currently in human clinical trials for a clinically unrelated indication. This drug showed activity against both major virulence factors, TcdA and TcdB, in biochemical and cell-based studies. Treatment in a mouse model of CDI that closely resembles the human infection confirmed a therapeutic benefit in the form of reduced disease pathology in host tissues that correlated with inhibition of the release of the toxic glucosyltransferase domain (GTD). Our results show that this non-antibiotic drug can modulate the pathology of disease and therefore could potentially be developed as a therapeutic for the treatment of CDI.**

INTRODUCTION

Clostridium difficile infection (CDI) is the leading cause of nosocomial diarrhea and the sole cause of pseudomembranous colitis (*1*). With a yearly average of over a quarter of a million hospitalizations in the United States alone (*2*), this infectious disease places an estimated burden of $4.8 billion on the U.S. health care system (*3*, *4*). Furthermore, the mortality rate in patients with CDI is high, with 6.9% at 30 days after diagnosis and 16.7% at 1 year after diagnosis (*4*). Skyrocketing numbers of cases in the past decade (139,000 in 2002 versus 453,000 in 2011), rising recurrence rates, and increasing numbers of strains resistant to almost all available antibiotics are creating a major public health threat (*5*, *6*). Only a handful of options are available to treat CDI infection, with antibiotics being the mainstay of clinical practice. Recurrence rates for CDI are as high as 25%, with most patients returning to the clinic for antibiotic treatment as soon as diarrhea recurs (*7*, *8*). By disrupting the growth cycle of bacteria, antibiotics rapidly select for antibiotic-resistant subpopulations (*9*). Hence, the rates of nosocomial infections caused by antibiotic-resistant opportunistic pathogens have more than doubled in the past decade (*10*, *11*). Although fecal bacteriotherapy has proven to be an extremely effective CDI treatment (*12*), it remains controversial from the perspective of drug regulation because the long-term effects on human health remain unclear (*13*).

A relatively unexplored strategy to combat bacterial pathogens is to block their ability to harm the host by directly inhibiting virulence factors (*14*). Such strategies would limit antibiotic use and, in turn, decrease the rate of emergence of resistant strains. Furthermore, in contrast to antibiotic treatment, targeting virulence factors may help to promote regrowth of commensal gut bacteria, a key factor in the clearance of CDI (*15*). The pathology of CDI is mediated by large clostridial toxins [toxins A (TcdA) and B (TcdB)]. Laboratory and epidemiological findings confirm that only toxigenic *C. difficile* causes disease (*16*, *17*) and that most disease-causing strains, including the epidemic and hypervirulent BI/NAP1/027 (*18*), carry the gene for TcdB (*19*). Both toxins are composed of a putative receptor binding domain, a transmembrane domain, a cysteine protease domain (CPD), and a glucosyltransferase domain (GTD) (*20*). When endocytosed by host cells and exposed to an acidic environment, the bacterial toxins undergo membrane translocation, exposing the CPD to the mammalian-specific cytosolic sugar 1D-myo-inositol hexakisphosphate (IP_6) (*21*). The allosteric binding of IP_6 activates the CPD to autocatalytically cleave the GTD domain, which induces toxicity by irreversible glucosylation of the Rho/Rac family of small guanosine triphosphatases (GTPases) in host intestinal epithelial cells. This event results in rearrangement of the actin cytoskeleton, acute inflammation, massive fluid secretion, and finally necrosis of the mucosal layer of the colon (*22*, *23*). However, it should be noted that recent findings showed that at high concentrations, toxin can cause cell necrosis in vitro in a translocation-dependent manner independent of its GTD activity (*24*) or autoprocessing mechanism (*22*). However, these in vitro phenomena have not been demonstrated in vivo, and it is not clear whether they play a role in the etiology of CDI. Necrosis within the mucosal layer results in typical CDI symptoms such as severe diarrhea and abdominal pain/tenderness (*25*). Severe cases of CDI are characterized by pseudomembranous colitis, perforations of the colon, and sepsis (*26*), and in acute situations, the mortality rate can be as high as 40% (*27*).

[1]Department of Pathology, Stanford University School of Medicine, 300 Pasteur Drive, Stanford, CA 94305–5324, USA. [2]Department of Microbiology and Immunology, Stanford University School of Medicine, Stanford, CA 94305–5124, USA. [3]Stanford University High-Throughput Bioscience Center, 1291 Welch Road, Stanford, CA 94305–5174, USA. [4]Division of Infectious Diseases and Geographic Medicine, Department of Medicine, Stanford University School of Medicine, Stanford, CA 94305–5107, USA. [5]Department of Microbiology and Molecular Genetics, University of Vermont, Burlington, VT 05405, USA.
*These authors contributed equally to this work.
†Present address: Department of Chemical Engineering, University of Washington, Seattle, WA 98195–1750 USA.
‡Corresponding author. E-mail: mbogyo@stanford.edu

Although the pathology of CDI is mediated by the large clostridial toxins, none of the currently available treatments target toxin activation, an event that requires allosteric regulation of the CPD domain to release the cytotoxic effector domain that mediates cytopathology and cytotoxicity. The only experimental therapy that targets these toxins is a monoclonal antibody combination of actoxumab and bezlotoxumab, which bind to the receptor binding [also known as combined repetitive oligopeptides (CROPs)] domains of TcdA and TcdB, respectively (*28*, *29*). Only in combination are these systemically delivered antibodies capable of neutralizing in vivo effects of clostridial toxins and suppressing the symptoms of disease (*30*). Here, we describe our efforts to identify small-molecule drug leads that target the activation of the toxins' CPD to further explore whether inhibition of proteolytic cleavage of the toxins could mitigate *C. difficile* pathology in vivo. Using a fluorescence polarization high-throughput screen, we identified a number of compounds that are potent inhibitors of CPD activity. One of the top hits was an existing investigational new drug in clinical trials called ebselen. We show that ebselen inhibits CPD activity in vitro and in vivo and has a beneficial effect on disease pathology in a mouse model of CDI.

RESULTS

Screening and in vitro validation identifies a potent inhibitor of TcdB CPD activation

Although most clinically isolated strains of *C. difficile* produce both TcdA and TcdB, TcdB seems to be the critical virulence factor of *C. difficile* (*31*–*33*), and its presence alone can cause CDI (*19*, *34*, *35*). When we analyzed the superimposed CPD crystal structures, the RMSD (spatial deviation between the structures) between the toxins was determined to be only 0.5 Å (Fig. 1A) (*36*), suggesting that the CPD domains of TcdA and TcdB are essentially identical in terms of their structural alignment (*37*). To identify small-molecule inhibitors of the CPD, we developed a fluorescence polarization high-throughput screen using the CPD from TcdB (Fig. 1C). This screen makes use of the fluorescent small-molecule activity-based probe TAMRA–AWP-19 (Fig. 1B), which covalently binds to the active-site cysteine residue of the CPD and reports on enzyme activity (*38*). With this probe, it is possible to screen for compounds that either inhibit or activate CPD protease activity in a high-throughput screen. We initially screened a library of bioavailable drugs considered clinically safe but without a U.S. Food and Drug Administration (FDA)–approved use, as well as the National Institutes of Health Clinical Collection. We identified a number of activators and inhibitors from both sets of compounds (table S1). This screen identified a total of 44 inhibitors, from which we selected a subset of preliminary hits that exhibited half maximal inhibitory concentrations (IC_{50}) lower than 7 μM. We used this set of compounds for further analysis in a cell rounding assay, where treatment of human foreskin fibroblast (HFF) cells with active full-length toxin induced cell rounding and eventual cell death (*39*). A concentration of TcdB that was sufficient to induce 100% cell rounding in 60 min was initially selected (fig. S1). This concentration of toxin was pretreated with our panel of inhibitors and coadministered to cells, with cell rounding visualized by microscopy. The assay identified a pool of compounds that demonstrated cytoprotective effects against the full-length toxin (fig. S2). When selecting a compound to advance into animal studies, we focused on candidates that had already been in clinical trials and therefore have greater potential for rapid translation to a human proof-of-principle trial. Of particular interest was a highly potent inhibitor, ebselen (2-phenyl-1,2-benzoselenazol-3-one) (Fig. 2A). This compound is currently in phase 2 clinical trials for the treatment of chemotherapy-induced hearing loss and as an otoprotectant for prevention of temporary auditory threshold shift (http://clinicaltrials.gov). Furthermore, a phase 2 clinical trial in Japan demonstrated that ebselen improved the outcome of patients suffering from an acute ischemic stroke (*40*).

Ebselen is a synthetic, low molecular weight organoselenium compound effective in reducing a variety of oxidative stress–mediated

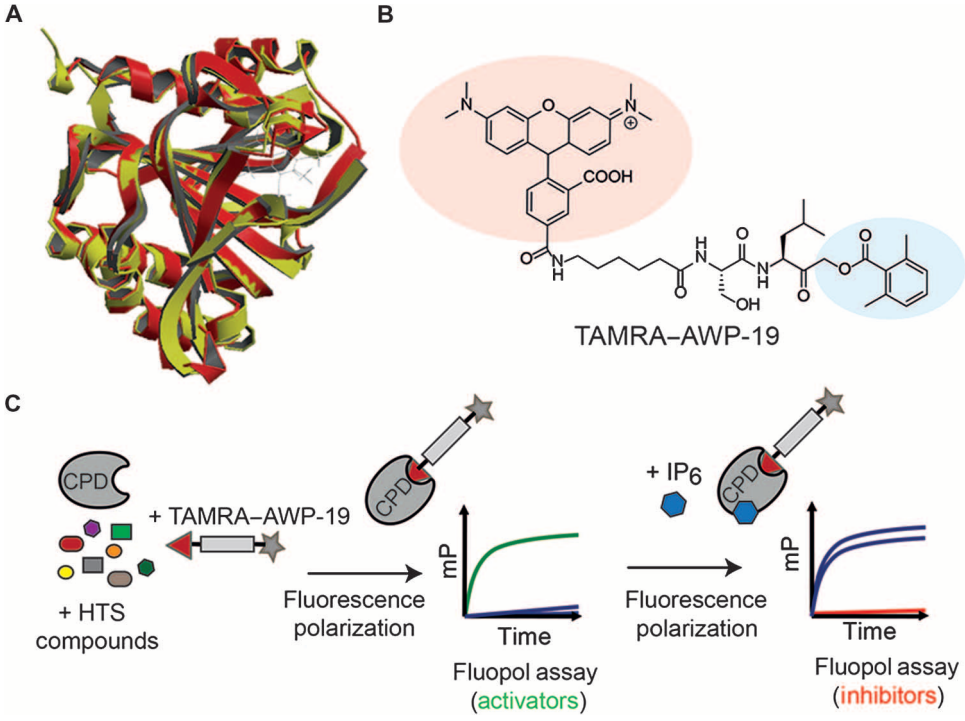

Fig. 1. Screening for small-molecule activators and inhibitors of the CPD of TcdB. (**A**) Superposition of the crystal structures of TcdB (red) and TcdA (yellow) CPD domains with an IP_6 allosteric activator bound. (**B**) Structure of the activity-based probe TAMRA–AWP-19 used for the high-throughput screen (HTS). The fluorophore is shaded in red, and the acyloxymethyl ketone electrophile specific for cysteine proteases is shown in blue. (**C**) Schematic of the fluorescence polarization (fluopol)–activity-based probe screen workflow. Compounds were added to the purified CPD domain from TcdB followed by addition of TAMRA–AWP-19 probe. The unbound probe produced low fluorescence polarization [millipolarization (mP)], which increased upon binding to the activated CPD. This change in millipolarization was measured on a plate reader and was used to assess the ability of a compound to either directly stimulate or inhibit (upon IP_6 addition) CPD activation.

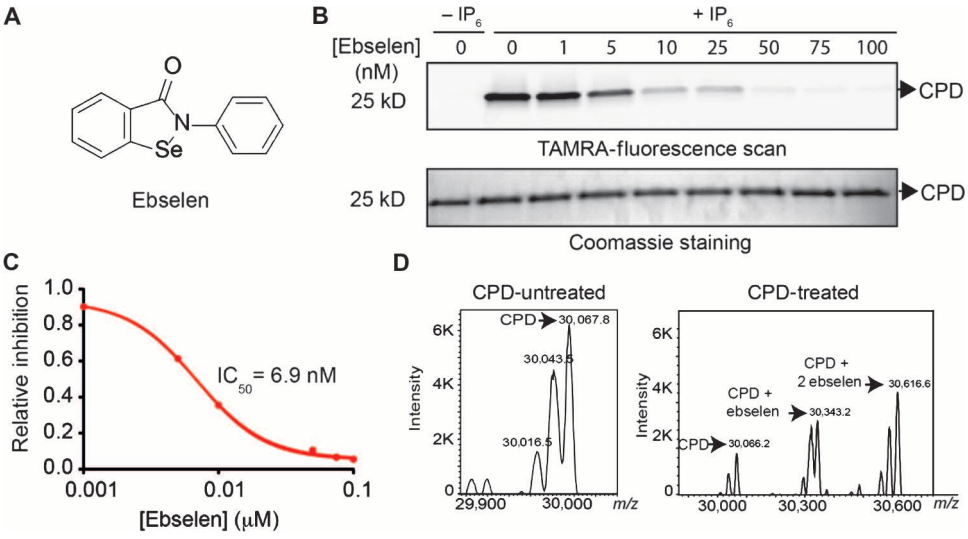

Fig. 2. Identification of ebselen as a potent inhibitor of CPD activation. (**A**) Chemical structure of the lead hit ebselen. (**B**) Assessment of CPD inhibition by labeling with TAMRA–AWP-19. The CPD was incubated with increasing amounts of ebselen, activated with IP_6, and labeled with TAMRA–AWP-19. Samples were resolved by SDS–polyacrylamide gel electrophoresis (SDS-PAGE) and scanned for probe fluorescence (top gel) or stained by Coomassie (bottom gel). (**C**) Dose-response curve of ebselen inhibition of the CPD as measured by quantification of probe labeling shown in (B). Values are plotted for percent inhibition relative to dimethyl sulfoxide (DMSO) control (lane 0). (**D**) Deconvoluted mass spectra of intact CPD (nondenaturing conditions) incubated with IP_6 (70 μM) with or without ebselen (100 nM) as indicated. The identified masses for the CPD plus ebselen addition are indicated.

pathologies in animal models and reported as a modifier of several unrelated bacterial virulence factors in vitro (*41*, *42*). It is reported to have glutathione peroxidase–like activity and reacts rapidly with peroxynitrite (a highly potent species that damages vital biomolecules) (*43*). The mechanism of action of ebselen involves changes of the oxidation state of the electrophilic selenium into selenol, which is then oxidized to selenic acid by reactive oxygen species (ROS), and finally reduced back to active selenol by glutathione through a selenylsulfide intermediate (*44*). It has been proposed, both in cellular systems and in vivo, that ebselen acts as an electrophilic modifier of plasma and intracellular proteins through selenosulfide conjugation with cysteine residues (*45*). Although the potential of ebselen to act as an enzyme inhibitor is somewhat unclear, selenium-containing compounds have been shown to act as inhibitors of cysteine proteases (*46*). We chose ebselen as our lead compound because it has a clean safety profile in humans, and human pharmacokinetic data are available, thus giving it high potential for clinical translation.

We began by performing detailed dose-response profiling studies of ebselen against the CPD domain and full-length toxin using a competition labeling assay with TAMRA–AWP-19. Ebselen inhibited IP_6-induced labeling of the CPD active-site cysteine (Fig. 2B) at low nanomolar concentrations (Fig. 2C). Deconvoluted mass spectrometry analysis confirmed the covalent modification of the CPD with one or two molecules of ebselen (Fig. 2D), consistent with modification of the CPD domain active-site cysteine and, unexpectedly, at an additional cysteine localized at the opposing surface of the CPD structure (*21*). Ebselen showed inhibition of IP_6-induced autoprocessing of both full-length TcdA and TcdB with low nanomolar potency (Fig. 3, A and B). These results also confirmed that ebselen completely inhibited the IP_6-induced release of the GTD at concentrations as low as 20 nM for TcdB, as measured by loss of the GTD fragment observed by Coomassie staining (Fig. 3B, bottom panel), with an IC_{50} for full-length TcdB inhibition of 17.2 nM (Fig. 3C).

To determine the molecular order of events for covalent modification of the CPD by ebselen, we tested whether covalent modification occurred before or after IP_6-induced allosteric activation. We treated full-length toxin with ebselen before or after the toxin was purified by size exclusion chromatography and before the addition of IP_6 (Fig. 3D). After addition of IP_6, the toxin was labeled with TAMRA–AWP-19 to assess inhibition. We observed inhibition of the labeling of the IP_6-activated toxin by TAMRA–AWP-19 only when the toxin was treated with ebselen after purification and IP_6 activation. This confirmed that covalent modification of the active site can only occur after allosteric activation of the toxin by IP_6 has taken place (Fig. 3E). It also confirmed that ebselen binding requires orientation of the active site by IP_6 and is not nonspecifically binding to free cysteine residues.

To determine the activity of ebselen in vitro, we performed a cell rounding assay (see fig. S1) with increasing concentrations of ebselen and then coadministered the TcdB/ebselen solution to cells (Fig. 4A). These data confirmed that the drug efficiently blocked cell rounding with an EC_{50} of 20.5 nM (Fig. 4B). Furthermore, when cells were preincubated with increasing concentrations of ebselen for 1 hour, washed, and subsequently challenged with toxin, we still observed a protective effect, with an EC_{50} of 217 nM (fig. S3). These data suggested that it is the intracellular pool of ebselen that provides protection against toxin-induced toxicity. To verify that the protective effect of ebselen on cells in the cell rounding assay was due to inhibition of release of the GTD domain, we performed Western blot analysis of the small Rho/Rac-GTPase substrates of the GTD. These data confirmed that the total population of Rac1 (measured by mAb23A8) remained stable across treatment groups, but the population of glucosylated Rac1 decreased with increasing amounts of ebselen (measured by detection of nonglucosylated Rac1 with mAb102) (Fig. 4C). Thus, ebselen blocks autoprocessing of TcdB, thereby inhibiting GTD-mediated irreversible glucosylation of Rho/Rac-GTPases. To confirm the potential clinical relevance of ebselen as a treatment for CDI, we tested its effects on cell rounding induced by the large clostridial toxins present in a stool sample obtained from a patient with CDI (fig. S4). In this clinical sample, where both TcdA and TcdB were present, ebselen efficiently inhibited toxin-induced cytopathology with an EC_{50} of 372 nM, consistent with our findings that ebselen blocks the activity of the purified toxins. Finally, to confirm that the effects of ebselen were mediated by its action on the CPD, we tested whether it had any direct inhibitory effect on the glucosyltransferase activity of the GTD domain. Using a commercial glucosyltransferase assay and a recombinantly expressed construct of the TcdB containing only the GTD domain (amino acids 1 to 543), we confirmed that ebselen did not show any inhibition of this activity at

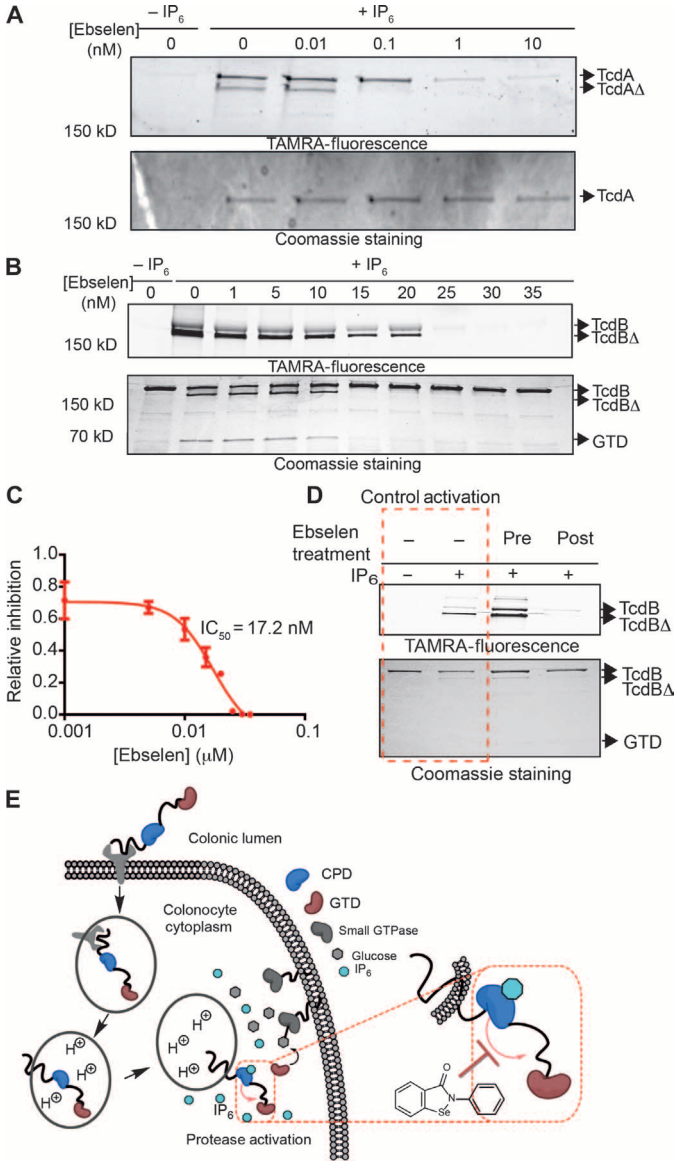

Fig. 3. Inhibition of full-length TcdA and TcdB by ebselen. (**A**) TcdA was incubated with increasing amounts of ebselen, activated with IP_6, and labeled with TAMRA–AWP-19. Samples were resolved by SDS-PAGE and scanned for probe fluorescence (top gel) or stained by Coomassie (bottom gel). Full-length TcdA and TcdA that has proteolytically released the GTD (TcdAΔ) are indicated by arrows. (**B**) TcdB was treated as in (A). Samples were resolved by SDS-PAGE and scanned for probe fluorescence (top gel) or stained by Coomassie (bottom gel). Full-length TcdB, TcdB that has proteolytically released the GTD (TcdBΔ), and the free GTD are indicated by arrows. The image shows a typical representation of three replicates. (**C**) Dose-response curve of ebselen inhibition of TcdB as measured by quantification of probe labeling as shown in (B). Values are plotted for percent inhibition relative to DMSO control (lane 0). (**D**) Uncoupling ebselen inhibition and IP_6 activation. Full-length TcdB was incubated with ebselen before (third lane) or after (fourth lane) size exclusion chromatography. Toxin was then activated with IP_6, labeled with TAMRA–AWP-19, and analyzed by SDS-PAGE and in-gel fluorescence analysis. Control lanes without ebselen treatment are marked in the red dashed box. All inhibition experiments were performed at least three times and, where applicable, represented as means ± SEM of triplicate analysis. (**E**) Proposed point of CPD inhibition mediated by ebselen (red dashed rectangle). Ebselen modifies the active-site cysteine upon IP_6-mediated allosteric activation in the cytosol.

concentrations about 1000-fold greater than the concentrations that protect against cell rounding in vitro (fig. S5).

Recent reports have demonstrated that the noncleavable L543A mutant and the catalytically inactive mutants C698S, H653A, and D587N of TcdB produce delayed toxicity in in vitro cell rounding assays and in a direct toxigenic mouse model of infection (*47*, *48*). Therefore, we examined the effects of ebselen over an extended time course on full-length TcdB wild-type and the L543A noncleavable mutant in the cell rounding assay. As reported in previously published studies, we observed a reduced and substantially delayed toxicity for the L543A mutant (Fig. 4D). This delayed toxicity was mimicked with nearly identical kinetics for the ebselen treatment of wild-type toxin, suggesting that ebselen's primary mode of action in the cell rounding assay is its ability to block cleavage and release of the GTD. Ebselen showed further protection against the delayed toxicity of the L543A mutant (Fig. 4D). Analysis of the full-length mutant toxin after IP_6 addition over the same extended time points revealed that the toxin undergoes IP_6-induced autoprocessing that can be blocked by the addition of ebselen (fig. S6). These results suggest that the delayed toxicity observed in the cell rounding assay for the mutant toxin is likely the result of release of the GTD through alternate processing by the CPD.

Ebselen treatment blocks the toxic effects of TcdB in vivo

To determine whether inhibition of TcdB by ebselen results in a loss of function of the toxin in vivo, we used the murine systemic intoxication model (*49*). A lethal dose of full-length TcdB (1.0 μg/kg) was pretreated with either DMSO or 100 nM ebselen for 1 hour, and then the mixture of toxin and drug was intraperitoneally injected into mice. Mice were monitored for 3 days for clinical signs of toxin action and eventual survival. Mice treated with ebselen had a 100% survival rate with no significant changes in vital signs (Fig. 4E), whereas the control group showed significant signs of toxicity (ruffled fur, decreased activity, peritoneal swelling, and hunched position) by 12 hours after toxin injection. The untreated group had a 60% mortality rate within the first 24 hours and a 100% mortality rate by the end of day 2 (Fig. 4F). Thus, inhibition of the CPD by ebselen efficiently blocked toxin function in vivo, resulting in complete protection from toxin lethality in this model.

Ebselen treatment reduces the pathology of *C. difficile* infection in mice

For a more clinically relevant test of the potential value of ebselen for the treatment of CDI, we performed a drug trial in a mouse model that closely mimics the human disease (*50*). To generate this model, mice were first exposed to a mixture of antibiotics (kanamycin, gentamicin, colistin, metronidazole, and vancomycin) for 3 days to compromise the colonization resistance typically afforded by the natural gut microbiota. After 2 days, mice were treated with clindamycin and, 24 hours later, challenged with *C. difficile* strain 630, a virulent and multidrug resistant strain of epidemic type X expressing the virulence factors TcdA and TcdB but not "binary toxin" (*51*, *52*). In this well-established model, mice develop symptoms including diarrhea and pathology in the cecum and colon that is consistent with that observed in human CDI, with a peak bacterial load 2 to 3 days after infection and symptoms

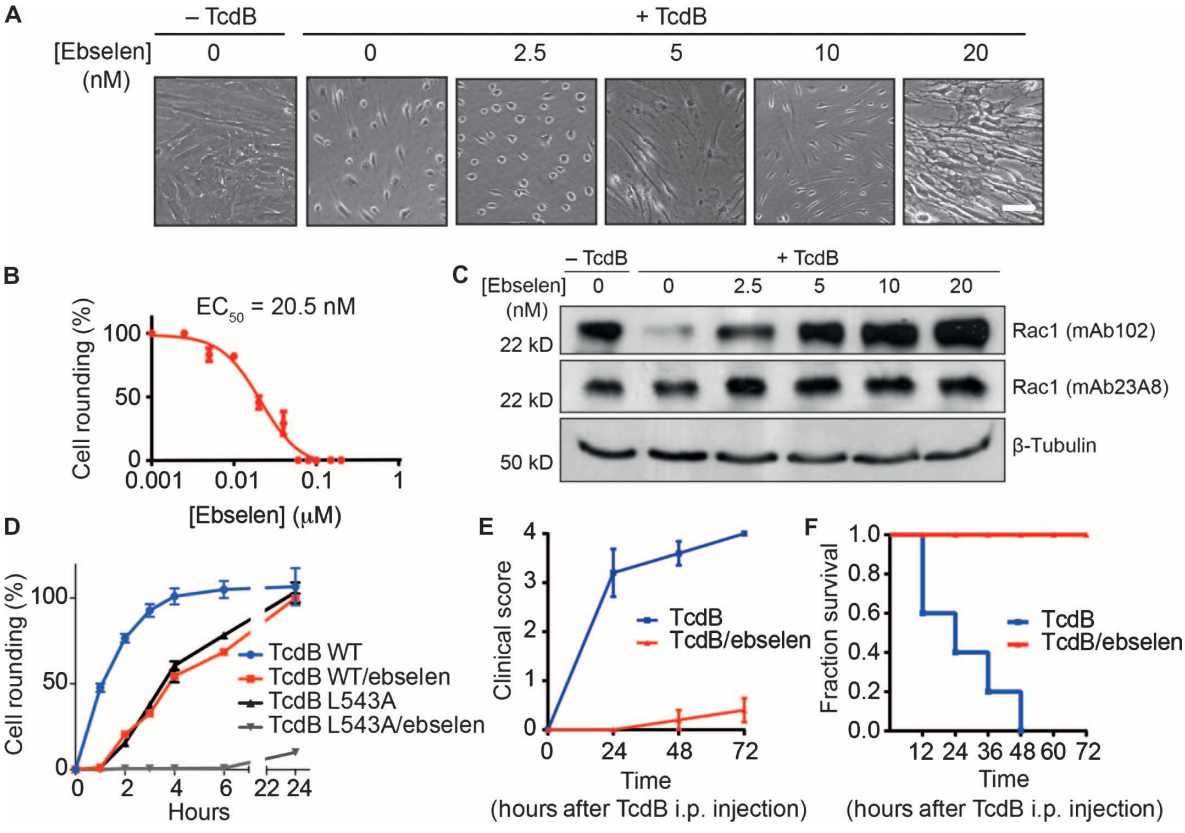

Fig. 4. Ebselen protects cells against TcdB-induced toxicity in vitro and in vivo. (**A**) HFF cells were challenged with DMSO, DMSO-treated TcdB, or TcdB treated with the indicated concentrations of ebselen. Images are representative fields for each sample. Scale bar, 10 μm. (**B**) EC_{50} values for cell rounding calculated by counting number of rounded cells and plotting as a percentage relative to the DMSO control. Results are means of three biological replicates ± SEM. (**C**) Western blot analysis of glucosyltransferase activity of TcdB in cell rounding assay. HFF cells were challenged as in (A), and cells were analyzed for total cellular Rac1 (mAb23A8, middle panel) and nonglucosylated Rac1 (mAb102, upper panel). β-Tubulin was used as a loading control (lower panel). Images are representative of three independent experiments. (**D**) Kinetic cell rounding assay of wild-type (WT) and noncleavable mutant toxin (L543A). HFF cells were challenged with 150 ng of full-length toxin (WT or L543A) that was preincubated with 100 nM ebselen or DMSO for 1 hour before coadministration to cells. Cell rounding was calculated as the percentage of rounded cells relative to DMSO-treated control cells at each time point. Results are means of three technical replicates ± SEM and representative of three independent experiments. (**E**) Mice (n = 5) were injected [intraperitoneally (i.p.)] with TcdB (1 μg/kg) or TcdB pretreated and coadministered with 100 nM ebselen. The plot shows clinical scores over time. Scores were assessed as follows: 0, healthy animal; 1, ruffled fur and BAR (bright, alert, and reactive); 2, ruffled fur, hunched, and QAR (quiet, alert, and reactive); 3, ruffled fur, hunched, inactive, and dehydrated; 4, moribund. Scores are plotted as the mean values for the five mice in each group ± SEM. (**F**) Survival plots showing the effect of ebselen treatment. Values were compiled using a Kaplan-Meier method using animals scored at 72 hours as the end point before humane termination. The χ^2 statistic was 10.90 with associated P value of <0.001.

continuing for 5 to 7 days (*53*, *54*). Throughout the course of disease (days 1 to 5), mice were treated daily with vehicle or ebselen (100 mg/kg) via oral gavage. This treatment regimen was chosen to mimic a hypothetical clinical scenario where high-risk patients (for example, hospitalized patients undergoing antibiotic treatment or patients with a history of *C. difficile* infection) could be treated prophylactically or upon occurrence of the first symptoms of *C. difficile* (diarrhea). Throughout the trial, fecal pellets were collected and used to determine the bacterial burden and to measure levels of TcdB-induced cell rounding activity of residually shed toxin. Ebselen treatment did not significantly affect the number of *C. difficile* colony-forming unit (CFU) counts throughout the 5-day experiment (Fig. 5A). This was expected because ebselen targets the toxic effects of TcdB and was not expected to grossly affect bacterial survival. However, we observed a reduction in cell rounding activity of shed toxin in terms of the quantity of feces required to induce 50% cell rounding [Fig. 5B, $^{**}P$ = 0.0043; fig. S7, P = 0.1170 (nonsignificant) for day 1, P = 0.1664 (nonsignificant) for day 2, P = 0.0110 (*) for day 3, and P = 0.0320 (*) for day 4], confirming that the activity of full-length toxin present in the fecal pellet was reduced. Western blot analysis of the colon tissues showed that ebselen treatment reduced the amount of the cleaved form of GTD when compared with vehicle-treated control group (Fig. 5F), confirming that ebselen was orally bioavailable in the colon and able to engage the intended target in vivo.

To assess the overall effects of ebselen on toxin-induced tissue pathology, we analyzed sections from the cecum and proximal colon of ebselen- and vehicle-treated mice by histopathological analysis at day 5 after infection (Fig. 5C). An independent pathologist, blinded to the tissue identities, scored the samples for inflammatory cell infiltration, submucosal edema, and mucosal hypertrophy, as well as for vascular congestion and epithelial disruption (*54*). Whereas none of the samples

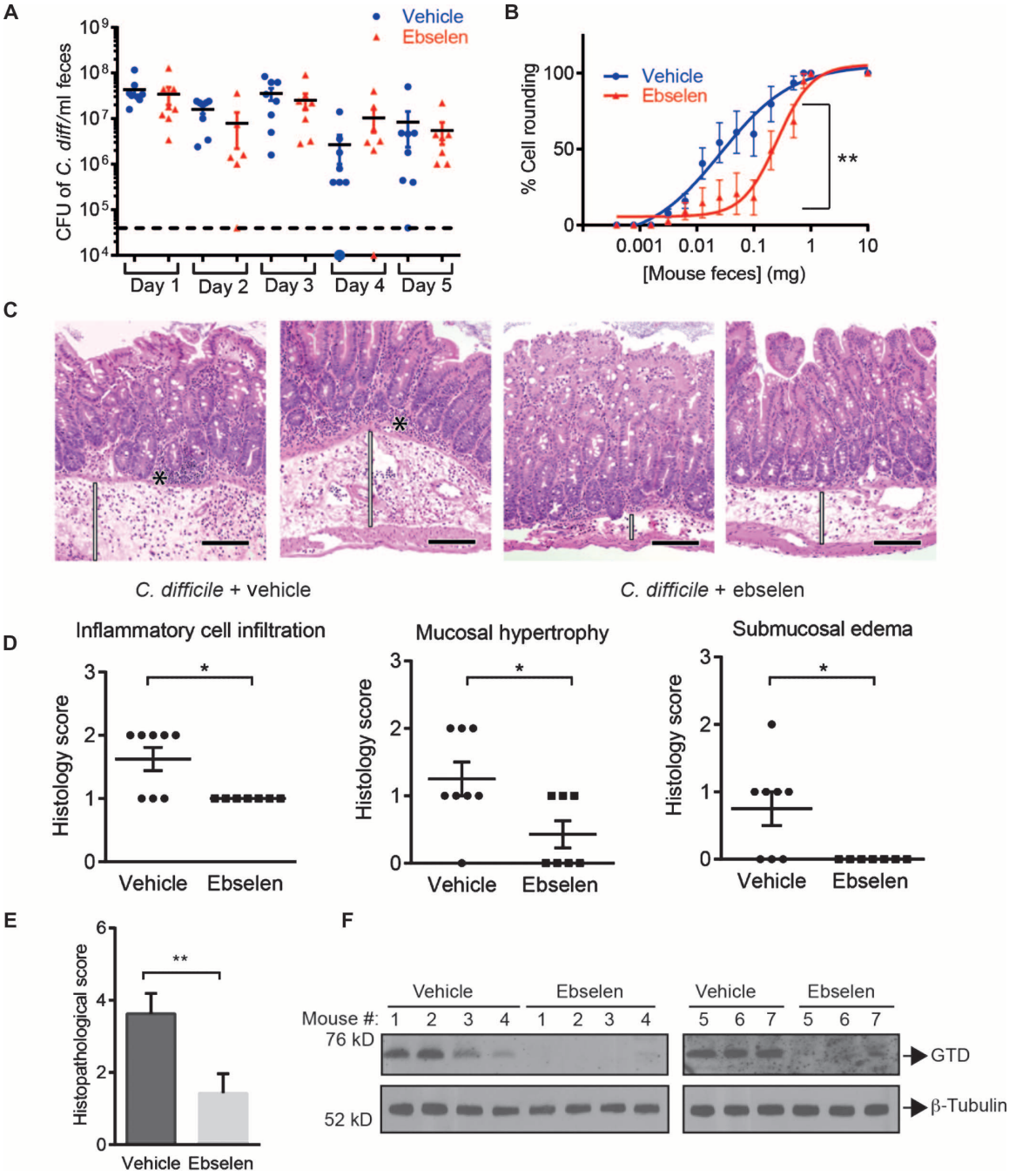

Fig. 5. Ebselen treatment blocks the pathology of *C. difficile* infection in mice. Mice were orally challenged with *C. difficile* (strain 630) and treated daily with vehicle or ebselen (100 mg/kg). (**A**) Plot of *C. difficile* CFU counts from fecal samples collected from ebselen- and vehicle-treated mice. (**B**) Plots showing the activity of TcdB in feces from vehicle- and ebselen-treated mice at day 5 after infection. The indicated milligram of feces equivalents collected from infected mice treated with ebselen (red, $n = 8$) or vehicle (blue, $n = 7$) were resuspended in 4× (w/v) phosphate-buffered saline (PBS) and applied to HFF cells. Cell rounding was calculated as the percentage of rounded cells relative to DMSO-treated control cells. Results are means ± SEM. Samples were statistically analyzed using paired *t* test. $^{**}P < 0.01$. (**C**) Images [hematoxylin and eosin (H&E) stain] of colon tissue sections from infected mice treated with vehicle or ebselen. Black asterisks indicate neutrophilic infiltration in the lamina propria of the mucosa. Expansion/thickening of the submucosa with edema and neutrophilic infiltrates are highlighted with white bars. Magnification, ×200. Black scale bars, 100 μm. (**D**) Histopathological scores for vehicle-treated (circles) and ebselen-treated (squares) animals for inflammatory cell infiltration, submucosal edema, and mucosal hypertrophy. $^{*}P < 0.05$ by Mann-Whitney *U* test. (**E**) Plot of the overall average histopathological scores for ebselen- and vehicle-treated animals. Statistical analysis was performed using the Mann-Whitney test. $^{**}P < 0.01$. (**F**) Western blot analysis of the released GTD in the colon tissues from mice treated with ebselen or vehicle (upper panel). β-Tubulin was used as a loading control (lower panel).

demonstrated signs of vascular or epithelial damage, the clinical scores for cell infiltration, submucosal edema, and mucosal hypertrophy were significantly lower in the ebselen-treated group in comparison to the vehicle-treated group (Fig. 5D: for mucosal hypertrophy, $*P = 0.0392$; for submucosal edema, $*P = 0.0177$; for inflammatory cell infiltration, $*P = 0.0162$). Overall, there was a statistically significant drop in clinical score (Fig. 5E, $**P = 0.0055$). These results demonstrate that inhibition of CPD activity by ebselen resulted in a significant reduction in disease pathology in vivo.

To further confirm the effects of ebselen on disease pathology, we performed a dose-response study using the same mouse infection model as described in the previous experiment (Fig. 6). By using a drug titration, it was possible to correlate the effects of ebselen in reducing disease pathology with its ability to block release of the GTD in infected tissues. We treated three groups of mice (five mice per group) with increasing doses of ebselen (1, 10, and 100 mg/kg daily) and compared outcomes to vehicle-treated and uninfected animals. After a 5-day treatment, the animals were sacrificed and the tissues were analyzed histopathologically (Fig. 6A). We also analyzed tissues for the presence of the cleaved GTD by Western blot (Fig. 6B). We observed a dose-dependent reduction of pathology in ebselen-treated animals, with 1 mg/kg showing no improvement in histopathological score, 10 mg/kg showing partial response, and 100 mg/kg showing virtually complete response (Fig. 6C). Western blot analysis for the cleaved GTD domain in colonic tissues confirmed the dose-dependent relationship between ebselen's inhibition of toxin activity and disease outcome, with reduced levels of cleaved GTD correlating directly with reduced pathology in the tissues, indicating that ebselen likely functions in vivo by blocking GTD release via CPD inhibition (Fig. 6D).

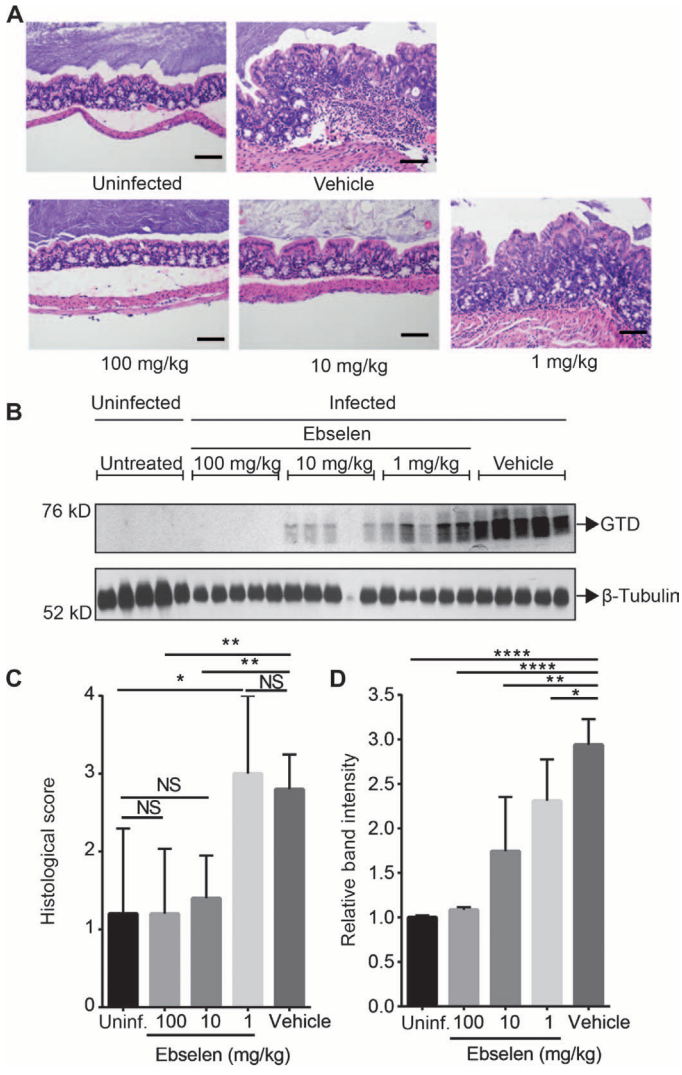

Fig. 6. Dose-dependent effects of ebselen on histopathology of *C. difficile* infection in mice. Antibiotic-pretreated mice were left untreated ($n = 5$) or orally challenged with *C. difficile* (strain 630) and treated daily with vehicle ($n = 5$) or ebselen at three doses [100 mg/kg ($n = 5$), 10 mg/kg ($n = 5$), and 1 mg/kg ($n = 5$)] for 5 days. (**A**) Representative images (H&E stain) of colon tissue sections from uninfected mice, infected mice treated with vehicle, or infected mice treated with ebselen at indicated doses. Black scale bars, 100 μm. (**B**) Western blot analysis of the released GTD in colon tissues from the uninfected mice or infected mice treated with vehicle or indicated doses of ebselen. β-Tubulin was used as a loading control. (**C**) Overall histopathological scores for uninfected or infected animals treated with vehicle or ebselen at the indicated doses. Statistical analysis was performed using the Mann-Whitney test. $**P < 0.01$, $*P < 0.05$; NS, nonsignificant. (**D**) Scanning densitometry of the Western blot images ($n = 5$ for each group). Results represent mean for each group of animals (uninfected; infected treated with ebselen at 100, 10, and 1 mg/kg; or infected treated with vehicle) ± SEM normalized to the signal for uninfected animals. All signals were normalized to β-tubulin. Statistical analysis was performed using Student's *t* test. $****P < 0.0001$, $**P < 0.01$, $*P < 0.05$.

DISCUSSION

CDI refers to a wide spectrum of diarrheal illnesses caused by the large clostridial toxins produced by *C. difficile*. With a marked rise in the number of cases of infection from hypervirulent strains, current antibiotic options are likely to soon become limited. Moreover, current first-line therapy of metronidazole followed by vancomycin poses an increased risk for the selection of resistant strains and promotes persistent overgrowth of other opportunistic enteric bacterial infections (*55*). Currently, any patient with a positive laboratory test for *C. difficile*, even when exhibiting mild symptoms, is treated with antibiotics when diagnosed (recommended clinical practice is a 10- to 14-day regimen of metronidazole) with more than 25% of infections recurring. Diarrhea is reported to recur at rates of up to 40% in patients with CDI and is usually the main reason that these patients return for antibiotic treatment (*56*). A growing body of evidence suggests that oral metronidazole and vancomycin cause disruption of the intestinal microflora, including *Bacteroides* species, which in turn promotes the overgrowth of nosocomial gastrointestinal pathogens (*55*). Thus, alternative clinical approaches that are less likely to disrupt the intestinal microbiota and that will help patients restore their natural gut commensals will be required. Fidaxomicin, a new class of macrocyclic antibiotic, is the only newly FDA-approved treatment for CDI in the past three decades and has a comparable efficacy profile to vancomycin in the treatment of the first onset of CDI with slightly lower rates of recurrence (*57*). Although fecal bacteriotherapy has proven to be extremely efficient, it remains controversial from a regulatory standpoint. Despite the fact that more than half a dozen companies are in the process of determining the individual species necessary for the recovery of a healthy microbiome in *C. difficile*–affected patients, it will most likely take significant time and investment for these tailored probiotic therapies to reach the clinic, and additional therapies

that can reduce the pathology of disease while such treatments are being administered will remain valuable.

Targeting the major virulence determinants of CDI pathology is a viable alternate strategy for treatment. Currently, neutralizing antibodies targeting the CROP domains of the toxin are in clinical trials, as well as combination antibodies against TcdA and TcdB. However, these agents are expensive to produce, have challenging manufacturing processes that often require additional preclinical and/or clinical testing to control variability and ensure compliance with quality standards, and demonstrate limitations in terms of their uptake (they have to be administered intravenously). Production costs for small-molecule agents are far less expensive and most can be optimized or formulated to be orally bioavailable. Our strategy was to determine the therapeutic potential of inhibiting toxin CPD activation by small molecules. These efforts identified ebselen, a drug with a proven safety profile in humans. Ebselen showed efficacy against autoproteolytic cleavage of both TcdA and TcdB, inhibited toxin-mediated pathology in vitro, blocked lethal toxicity of TcdB in a systemic toxigenic mouse model, and was efficacious in a clinically relevant mouse model of CDI.

Recently, multiple publications using mutants of TcdA and TcdB, including the noncleavable TcdA mutant $Ala^{541}Gly^{542}Ala^{543}$ as well as TcdB mutants L543A, C698S, H653A, and D587N, have shown delayed in vitro toxicity, leading to the suggestion that CPD-mediated intracellular cleavage is not essential to induce intoxication of host tissues (*22*, *47*, *48*, *58*). Here, we show that ebselen protects cells against TcdB in a cell rounding assay to a similar level of delayed potency induced by the noncleavable but catalytically active TcdB mutant L543A. These results suggest that the protective effect of ebselen is mediated by its ability to block CPD-mediated processing of the GTD. Further, ebselen protected against TcdB mutant L543A-induced cell rounding, suggesting that it may be blocking CPD-mediated proteolytic cleavage of a nonpreferred alternate cleavage site of TcdB or that the CPD plays additional roles in the overall intoxication process beyond cleavage of the GTD. Thus, by simply blocking GTD release but not blocking the CPD activity, there is residual toxicity. Regardless of our current results using the mutant toxins, it should be noted that these studies make use of purified toxin applied to cells under controlled conditions in vitro. Furthermore, in vivo studies of the noncleavable mutant TcdB have only been performed using purified toxin in a toxigenic model that also fails to recapitulate a clinically relevant infection by the intact pathogen. Thus, all of the current results using mutant toxins must be considered with some degree of caution with respect to their relevance to human infection by *C. difficile*. Our results showing delayed toxicity of the purified toxin in vitro upon ebselen treatment yet complete protection that correlates with the extent of GTD release in the relevant infection model in vivo suggest that the "residual" in vitro toxicity of mutant toxins may have little relevance to the pathology observed in CDI. Further studies using a *C. difficile* strain that has been engineered to produce only the catalytically inactive CPD of both TcdA and TcdB will be required to ultimately confirm the relevance of the in vitro data using the mutant toxins.

Although our combined results strongly suggest that ebselen functions by blocking GTD release, recent findings demonstrating that toxin-induced cell death is dependent on ROS (*23*) raise the possibility that ebselen could also confer some level of protection via its antioxidant effect. We cannot completely rule out that the improvement in pathology could be partially contributed by ebselen-mediated neutralization of ROS formed by the inflammatory response during the course of *C. difficile* infection. Although this study could not uncouple any potential antioxidant functions of ebselen from its effects on the CPD domain, any added antioxidant effects of ebselen would serve to enhance the efficacy of the drug by using multiple mechanisms to generate therapeutic benefit.

Another limitation in this study and the mouse model used is its inability to allow assessment of recurrence rates. This mouse model of CDI was chosen because it most closely mimics the initial onset of human disease. However, because the model is not persistent and the mice eventually recover from infection, analysis of the effects of ebselen is limited to the initial infection. Additionally, this study did not assess the potential of ebselen to allow recovery of the microbiota that naturally prevents *C. difficile* from colonizing the gastrointestinal tract. This is an important area for future study because one of most significant benefits of using a non-antibiotic treatment would be its ability to allow return of the natural gut microbiome.

In addition, we chose to treat mice with ebselen 2 hours before infection to most optimally assess the effect of the drug on toxin-mediated pathology. This experimental design is clinically relevant because it models prophylactic treatment of patients who are at high risk for CDI infection, such as those taking antibiotics for an unrelated bacterial infection.

Despite the limitations in this study, as a monotherapeutic or as a complement to first-line antibiotics, ebselen may ameliorate not only the symptoms of initial onset of CDI but also potentially lower the recurrence rate and play a beneficial role in the restoration of the natural microbiota in patients. The remaining challenges for clinical translation of ebselen will be developing methods to optimize oral delivery of the drug to the site of action of the bacterial toxins, although this should be possible by using drug formulations that allow slow release of the compound in the colon where it can continuously act on the toxin as it is produced and secreted by the pathogen. However, on the basis of existing pharmacokinetics data for ebselen in humans, effectiveness may be achieved in its current oral formulation, thus greatly accelerating the time to initiation of a clinical trial. These studies warrant continued efforts toward the clinical translation of ebselen for the treatment of CDI.

MATERIALS AND METHODS

Study design

This study sought to identify potential new antivirulence therapeutic agents that target the CPD of TcdA and TcdB of *C. difficile*. The top lead compound ebselen was assessed as a potential therapeutic in vivo using a toxigenic model of infection and a mouse model of CDI. Efficacy in vivo was determined on the basis of morbidity, cell rounding of residually shed toxin in fecal material, release of the toxic GTD domain of TcdB, and histopathological score of cecum and colon tissue samples. Sample size of animals used for in vivo experiments was determined on the basis of the estimates of the means and indications of the likely responses. Animals were assigned to each experimental group with an equal probability of receiving vehicle or treatment. To avoid potential bias and subjective elements in assessing the results, histopathological scoring experiments were performed by a pathologist blinded to the identity of the samples.

Protein expression and purification

The TcdB CPD domain was expressed and purified according to Shen *et al.* (*21*). The full-length TcdB expression vector was a gift from

D. Borden Lacy (Vanderbilt University, Nashville, TN). The expression of this construct was performed according to Yang *et al.* (*59*). GTD domain constructs were cloned into pET28a vectors (Supplementary Materials and Methods).

Cell rounding assay

HFFs, cultured in Dulbecco's modified medium [supplemented with 10% (v/v) fetal calf serum, penicillin (100 μg/ml), and 100 mM streptomycin], were plated in 24-well dishes and grown to confluency. Cells were treated with TcdB (100 pM final concentration in 1 ml of medium) that was pretreated with DMSO or with increasing amounts of ebselen (diluted from 20× stock solutions) for 60 min in 15 μl of CPD buffer. Control cells were treated with the reaction vehicle (CPD buffer with 0.75 μl of DMSO) and treated with the same amount of toxin or buffer control. Rounded cells were counted using a Leica microscope eyepiece counting grid and expressed as percentage of total cells. Specific experimental protocols are detailed in Supplementary Materials and Methods.

Bacterial strains and culture conditions

C. difficile strain 630 was used in all experiments and was cultured in Brain Heart Infusion medium (Becton Dickinson) supplemented with yeast extract (Remel) (5 mg/ml) anaerobically (6% H_2, 20% CO_2, 74% N_2). For quantification of *C. difficile* CFU counts in conventional mice, 1 μl of feces was serially diluted in PBS and plated onto *C. difficile* moxalactam norfloxacin plates composed of *C. difficile* agar base (Oxoid) with 7% (v/v) of defibrinated horse blood (Lampire Biological Laboratories), supplemented with moxalactam (32 mg/μl) (Santa Cruz Biotechnology) and norfloxacin (12 mg/μl) (Sigma-Aldrich). Plates were incubated overnight at 37°C in an anaerobic chamber (Coy).

Mouse toxigenic model

Mouse TcdB toxigenic experiments were performed according to Administrative Panel on Laboratory Animal Care (A-PLAC) protocols approved by Stanford Institutional Animal Care and Use Committee (IACUC). The toxigenic model was adapted from Lanis *et al.* (*49*). Full-length toxin was sterilely filtered using Corning Costar Spin-X Centrifugal Filter Devices (with 0.22-μm pore diameter) to ensure that the injection is not painful to the animals and does not cause abscess. Two groups of mice (ebselen- and control-treated) were intraperitoneally injected with TcdB (1 μg of toxin/kg, in a volume of 100 μl) pretreated with 100 nM ebselen or DMSO for 1 hour. Mice were monitored for toxicity and scored using the following clinical score: 0, healthy animal; 1, ruffled fur and BAR (bright, alert, and reactive); 2, ruffled fur, hunched, and QAR (quiet, alert, and reactive); 3, ruffled fur, hunched, inactive, and dehydrated; 4, moribund (rapid breathing, hemiparesis, tachypneic state, grimacing, hypothermia, peritoneal swelling, hunched inactive, and dehydrated). Mice scored at 4 were sacrificed according to the A-PLAC protocol and considered as the "mortality" end point population in the study. Survival plots were created using GraphPad Prism 6.0 with death as the point when moribund animals were scored at clinical score 4 (time of sacrifice).

Mouse *C. difficile* infection model

Conventional Swiss-Webster mice (RFSW, Taconic) were maintained in accordance with A-PLAC protocols approved by the Stanford IACUC. Before *C. difficile* challenge, antibiotics [kanamycin (0.4 mg/ml), gentamicin (0.035 mg/ml), colistin (850 U/ml), metronidazole (0.215 mg/ml), and vancomycin (0.045 mg/ml)] were administered in drinking water for 3 days, starting 6 days before inoculation as previously reported (*50*). Mice were switched to regular water for 2 days and then administered with 1 mg of clindamycin via oral gavage 1 day before *C. difficile* (strain 630) inoculation (10^8 CFU from overnight cultures via oral gavage). Mouse feces used for CFU counts and cell rounding assays were collected daily before oral gavages with ebselen.

Ebselen treatment

Mice (eight ebselen-treated and seven vehicle-treated) with an average weight of 30 g were treated starting with the first dose 2 hours before *C. difficile* challenge, followed by daily gavages with ebselen at 2:00 p.m. for 4 days. The daily dose of ebselen was 100 mg/kg in a 200-μl final volume. The compound was dissolved in DMSO and then resuspended in a 1:4 (v/v) DMSO/oil microemulsion to a final concentration of 15 mg/ml. The control group was treated with vehicle only. Mice were sacrificed according to the guidelines on humane termination 5 days after infection. Colon tissues were collected for histological analysis.

Dose-response of ebselen in vivo

Twenty-five mice undergoing the same antibiotic regimen as described above were uninfected (n = 5, uninfected control) or infected with *C. difficile* (n = 20). Infected animals were divided into four different groups and treated with (i) ebselen at 100 mg/kg, (ii) ebselen at 10 mg/kg, (iii) ebselen at 1 mg/kg, and (iv) vehicle (6.7% DMSO, 1% Tween 80 in PBS) starting with the first dose 2 hours before *C. difficile* challenge, followed by daily gavages for 4 days. Mice were sacrificed according to the guidelines on humane termination 5 days after infection, and the colonic tissues were collected for histological analysis.

Histochemistry and histopathological scoring

Proximal colon and cecum sections were collected and fixed in 10% formalin for 24 hours and then stored in 70% ethanol. Cassettes were paraffin-embedded, sectioned, mounted on slides, and stained with the H&E stain (Histo-Tec Laboratory). Histological specimens were scored by veterinarian pathologists blinded to the identity of the histological sections [R. Luong, Stanford Veterinary Service Center, and D. Imai, University of California (UC), Davis]. The scoring system was adapted from Pawlowski *et al.* (*54*) with the scale being 0 to 3 (minimal score, 0; maximal score, 3) and included the following pathological features: inflammatory cell infiltration, mucosal hypertrophy, vascular congestion, epithelial disruption, and submucosal edema.

Statistical analyses

Histopathological, biochemical, and in vitro data were analyzed using GraphPad Prism 6.0 (GraphPad Software Inc.) and expressed as means ± SEM. Statistical analyses were performed using the Student's t test unless stated otherwise. P values less than or equal to 0.05 were considered significant.

SUPPLEMENTARY MATERIALS

www.sciencetranslationalmedicine.org/cgi/content/full/7/306/306ra148/DC1

Materials and Methods

Fig. S1. TcdB-induced cell rounding in HFF cells.

Fig. S2. Efficacy of TcdB inhibitors in biochemical and cell-based assays.

Fig. S3. Ebselen protects cells against TcdB-induced toxicity in vitro.

Fig. S4. Ebselen inhibits toxin-induced cytopathic effect in a fecal sample from a *C. difficile* patient.

Fig. S5. Effect of ebselen on the GTD domain of TcdB.

Fig. S6. Ebselen protects against autoprocessing of full-length wild-type and L543A toxin over time.
Fig. S7. Dose-response plots showing the activity of TcdB in feces of vehicle- and ebselen-treated mice from days 1 to 4 after *C. difficile* infection.
Table S1. List of TcdB CPD inhibitors with corresponding IC_{50} values obtained from the fluorescence polarization high-throughput screen.
Table S2. Primary data supporting Fig. 4E.
Table S3. Primary data supporting Fig. 4F.
Table S4. Primary data supporting Fig. 5 (D and E).
Table S5. Primary data supporting Fig. 6C.
References (*60*–*64*)

REFERENCES AND NOTES

1. C. M. Surawicz, L. J. Brandt, D. G. Binion, A. N. Ananthakrishnan, S. R. Curry, P. H. Gilligan, L. V. McFarland, M. Mellow, B. S. Zuckerbraun, Guidelines for diagnosis, treatment, and prevention of *Clostridium difficile* infections. *Am. J. Gastroenterol.* **108**, 478–498 (2013).
2. Center for Disease Control and Prevention, *Antibiotic Resistance Threats in the United States 2013* (CDC, Atlanta, GA, 2013).
3. R. Douglas Scott II, *The Direct Medical Costs of Healthcare-Associated Infections in U.S. Hospitals and the Benefits of Prevention, Division of Healthcare Quality Promotion National Center for Preparedness, Detection, and Control of Infectious Diseases. Coordinating Center for Infectious Diseases* (CDC, Atlanta, GA, 2009).
4. E. R. Dubberke, M. A. Olsen, Burden of *Clostridium difficile* on the healthcare system. *Clin. Infect. Dis.* **55**, S88–S92 (2012).
5. M.-C. Tran, M. C. Claros, E. J. Goldstein, Therapy of *Clostridium difficile* infection: Perspectives on a changing paradigm. *Expert Opin. Pharmacother.* **14**, 2375–2386 (2013).
6. F. C. Lessa, Y. Mu, W. M. Bamberg, Z. G. Beldavs, G. K. Dumyati, J. R. Dunn, M. M. Farley, S. M. Holzbauer, J. I. Meek, E. C. Phipps, L. E. Wilson, L. G. Winston, J. A. Cohen, B. M. Limbago, S. K. Fridkin, D. N. Gerding, L. C. McDonald, Burden of *Clostridium difficile* infection in the United States. *N. Engl. J. Med.* **372**, 825–834 (2015).
7. C. P. Kelly, Can we identify patients at high risk of recurrent *Clostridium difficile* infection? *Clin. Microbiol. Infect.* **18**, 21–27 (2012).
8. M. Y. Hu, K. Katchar, L. Kyne, S. Maroo, S. Tummala, V. Dreisbach, H. Xu, D. A. Leffler, C. P. Kelly, Prospective derivation and validation of a clinical prediction rule for recurrent *Clostridium difficile* infection. *Gastroenterology* **136**, 1206–1214 (2009).
9. C. Walsh, *Antibiotics: Actions, Origins, Resistance* (ASM Press, Washington, DC, 2003).
10. C. A. Arias, B. E. Murray, The rise of the *Enterococcus*: Beyond vancomycin resistance. *Nat. Rev. Microbiol.* **10**, 266–278 (2012).
11. A. M. Ramsey, M. D. Zilberberg, Secular trends of hospitalization with vancomycin-resistant *Enterococcus* infection in the United States, 2000–2006. *Infect. Control Hosp. Epidemiol.* **30**, 184–186 (2009).
12. E. van Nood, A. Vrieze, M. Nieuwdorp, S. Fuentes, E. G. Zoetendal, W. M. de Vos, C. E. Visser, E. J. Kuijper, J. F. Bartelsman, J. G. Tijssen, P. Speelman, M. G. Dijkgraaf, J. J. Keller, Duodenal infusion of donor feces for recurrent *Clostridium difficile*. *N. Engl. J. Med.* **368**, 407–415 (2013).
13. E. G. Pamer, Fecal microbiota transplantation: Effectiveness, complexities, and lingering concerns. *Mucosal Immunol.* **7**, 210–214 (2014).
14. P. F. Vale, A. Fenton, S. P. Brown, Limiting damage during infection: Lessons from infection tolerance for novel therapeutics. *PLOS Biol.* **12**, e1001769 (2014).
15. Y. Taur, E. G. Pamer, Harnessing microbiota to kill a pathogen: Fixing the microbiota to treat *Clostridium difficile* infections. *Nat. Med.* **20**, 246–247 (2014).
16. J. K. Shim, S. Johnson, M. H. Samore, D. Z. Bliss, D. N. Gerding, Primary symptomless colonisation by *Clostridium difficile* and decreased risk of subsequent diarrhoea. *Lancet* **351**, 633–636 (1998).
17. L. Kyne, M. Warny, A. Qamar, C. P. Kelly, Asymptomatic carriage of *Clostridium difficile* and serum levels of IgG antibody against toxin A. *N. Engl. J. Med.* **342**, 390–397 (2000).
18. J. R. O'Connor, S. Johnson, D. N. Gerding, *Clostridium difficile* infection caused by the epidemic BI/NAP1/027 strain. *Gastroenterology* **136**, 1913–1924 (2009).
19. D. Drudy, N. Hamedy, S. Fanning, M. Hannan, L. Kyne, Emergence and control of fluoroquinolone-resistant, toxin A–negative, toxin B–positive *Clostridium difficile*. *Infect. Control Hosp. Epidemiol.* **28**, 932–940 (2007).
20. R. N. Pruitt, D. B. Lacy, Toward a structural understanding of *Clostridium difficile* toxins A and B. *Front. Cell. Infect. Microbiol.* **2**, 28 (2012).
21. A. Shen, P. J. Lupardus, M. M. Gersch, A. W. Puri, V. E. Albrow, K. C. Garcia, M. Bogyo, Defining an allosteric circuit in the cysteine protease domain of *Clostridium difficile* toxins. *Nat. Struct. Mol. Biol.* **18**, 364–371 (2011).
22. N. M. Chumbler, M. A. Farrow, L. A. Lapierre, J. L. Franklin, D. B. Haslam, J. R. Goldenring, D. B. Lacy, *Clostridium difficile* toxin B causes epithelial cell necrosis through an autoprocessing-independent mechanism. *PLOS Pathog.* **8**, e1003072 (2012).
23. M. A. Farrow, N. M. Chumbler, L. A. Lapierre, J. L. Franklin, S. A. Rutherford, J. R. Goldenring, D. B. Lacy, *Clostridium difficile* toxin B-induced necrosis is mediated by the host epithelial cell NADPH oxidase complex. *Proc. Natl. Acad. Sci. U.S.A.* **110**, 18674–18679 (2013).
24. Z. Zhang, M. Park, J. Tam, A. Auger, G. L. Beilhartz, D. B. Lacy, R. A. Melnyk, Translocation domain mutations affecting cellular toxicity identify the *Clostridium difficile* toxin B pore. *Proc. Natl. Acad. Sci. U.S.A.* **111**, 3721–3726 (2014).
25. B. A. Feltis, S. M. Wiesner, A. S. Kim, S. L. Erlandsen, D. L. Lyerly, T. D. Wilkins, C. L. Wells, *Clostridium difficile* toxins A and B can alter epithelial permeability and promote bacterial paracellular migration through HT-29 enterocytes. *Shock* **14**, 629–634 (2000).
26. S. R. Eaton, J. E. Mazuski, Overview of severe *Clostridium difficile* infection. *Crit. Care Clin.* **29**, 827–839 (2013).
27. J. Pépin, L. Valiquette, B. Cossette, Mortality attributable to nosocomial *Clostridium difficile*–associated disease during an epidemic caused by a hypervirulent strain in Quebec. *CMAJ* **173**, 1037–1042 (2005).
28. G. J. Babcock, T. J. Broering, H. J. Hernandez, R. B. Mandell, K. Donahue, N. Boatright, A. M. Stack, I. Lowy, R. Graziano, D. Molrine, D. M. Ambrosino, W. D. Thomas Jr., Human monoclonal antibodies directed against toxins A and B prevent *Clostridium difficile*-induced mortality in hamsters. *Infect. Immun.* **74**, 6339–6347 (2006).
29. Z. Yang, J. Ramsey, T. Hamza, Y. Zhang, S. Li, H. G. Yfantis, D. Lee, L. Hernandez, W. Seghezzi, J. M. Furneisen, N. M. Davis, A. G. Therien, H. Feng, Mechanisms of protection against *Clostridium difficile* infection by the monoclonal antitoxin antibodies actoxumab and bezlotoxumab. *Infect. Immun.* **83**, 822–831 (2015).
30. I. Lowy, D. C. Molrine, B. A. Leav, B. M. Blair, R. Baxter, D. N. Gerding, G. Nichol, W. D. Thomas Jr., M. Leney, S. Sloan, C. A. Hay, D. M. Ambrosino, Treatment with monoclonal antibodies against *Clostridium difficile* toxins. *N. Engl. J. Med.* **362**, 197–205 (2010).
31. S. A. Kuehne, S. T. Cartman, J. T. Heap, M. L. Kelly, A. Cockayne, N. P. Minton, The role of toxin A and toxin B in *Clostridium difficile* infection. *Nature* **467**, 711–713 (2010).
32. D. Lyras, J. R. O'Connor, P. M. Howarth, S. P. Sambol, G. P. Carter, T. Phumoonna, R. Poon, V. Adams, G. Vedantam, S. Johnson, D. N. Gerding, J. I. Rood, Toxin B is essential for virulence of *Clostridium difficile*. *Nature* **458**, 1176–1179 (2009).
33. J. D. Ballard, Medical microbiology: A toxin contest. *Nature* **467**, 665–666 (2010).
34. S. Janezic, M. Marín, A. Martín, M. Rupnik, A new type of toxin A-negative, toxin B-positive *Clostridium difficile* strain lacking a complete *tcdA* gene. *J. Clin. Microbiol.* **53**, 692–695 (2015).
35. B. Elliott, M. M. Squire, S. Thean, B. J. Chang, J. S. Brazier, M. Rupnik, T. V. Riley, New types of toxin A-negative, toxin B-positive strains among clinical isolates of *Clostridium difficile* in Australia. *J. Med. Microbiol.* **60**, 1108–1111 (2011).
36. R. Maiti, G. H. Van Domselaar, H. Zhang, D. S. Wishart, SuperPose: A simple server for sophisticated structural superposition. *Nucleic Acids Res.* **32**, W590–W594 (2004).
37. M. Egerer, T. Giesemann, T. Jank, K. J. F. Satchell, K. Aktories, Auto-catalytic cleavage of *Clostridium difficile* toxins A and B depends on cysteine protease activity. *J. Biol. Chem.* **282**, 25314–25321 (2007).
38. A. W. Puri, P. J. Lupardus, E. Deu, V. E. Albrow, K. C. Garcia, M. Bogyo, A. Shen, Rational design of inhibitors and activity-based probes targeting *Clostridium difficile* virulence factor TcdB. *Chem. Biol.* **17**, 1201–1211 (2010).
39. M. J. Gurwith, C. Langston, B. Dunsmore, Morphologic and functional effects of *Clostridium difficile* enterotoxin in tissue culture. *Can. J. Microbiol.* **28**, 100–105 (1982).
40. T. Yamaguchi, K. Sano, K. Takakura, I. Saito, Y. Shinohara, T. Asano, H. Yasuhara, Ebselen in acute ischemic stroke: A placebo-controlled, double-blind clinical trial. Ebselen Study Group. *Stroke* **29**, 12–17 (1998).
41. L. Favrot, A. E. Grzegorzewicz, D. H. Lajiness, R. K. Marvin, J. Boucau, D. Isailovic, M. Jackson, D. R. Ronning, Mechanism of inhibition of *Mycobacterium tuberculosis* antigen 85 by ebselen. *Nat. Commun.* **4**, 2748 (2013).
42. O. J. Lieberman, M. W. Orr, Y. Wang, V. T. Lee, High-throughput screening using the differential radial capillary action of ligand assay identifies ebselen as an inhibitor of diguanylate cyclases. *ACS Chem. Biol.* **9**, 183–192 (2014).
43. K. P. Bhabak, G. Mugesh, Functional mimics of glutathione peroxidase: Bioinspired synthetic antioxidants. *Acc. Chem. Res.* **43**, 1408–1419 (2010).
44. T. Sakurai, M. Kanayama, T. Shibata, K. Itoh, A. Kobayashi, M. Yamamoto, K. Uchida, Ebselen, a seleno-organic antioxidant, as an electrophile. *Chem. Res. Toxicol.* **19**, 1196–1204 (2006).
45. G. K. Azad, R. S. Tomar, Ebselen, a promising antioxidant drug: Mechanisms of action and targets of biological pathways. *Mol. Biol. Rep.* **41**, 4865–4879 (2014).
46. L. Piovan, M. F. M. Alves, L. Juliano, D. Brömme, R. L. O. R. Cunha, L. H. Andrade, Chemoenzymatic synthesis of organoselenium(IV) compounds and their evaluation as cysteine protease inhibitors. *J. Braz. Chem. Soc.* **21**, 2108–2118 (2010).
47. S. Li, L. Shi, Z. Yang, Y. Zhang, G. Perez Cordon, T. Huang, J. Ramsey, N. Oezguen, T. C. Savidge, H. Feng, Critical roles of *Clostridium difficile* toxin B enzymatic activities in pathogenesis. *Infect. Immun.* **83**, 502–513 (2015).
48. S. Li, L. Shi, Z. Yang, H. Feng, Cytotoxicity of *Clostridium difficile* toxin B does not require cysteine protease-mediated autocleavage and release of the glucosyltransferase domain into the host cell cytosol. *Pathog. Dis.* **67**, 11–18 (2013).
49. J. M. Lanis, L. D. Heinlen, J. A. James, J. D. Ballard, *Clostridium difficile* 027/BI/NAP1 encodes a hypertoxic and antigenically variable form of TcdB. *PLOS Pathog.* **9**, e1003523 (2013).

50. K. M. Ng, J. A. Ferreyra, S. K. Higginbottom, J. B. Lynch, P. C. Kashyap, S. Gopinath, N. Naidu, B. Choudhury, B. C. Weimer, D. M. Monack, J. L. Sonnenburg, Microbiota-liberated host sugars facilitate post-antibiotic expansion of enteric pathogens. *Nature* **502**, 96–99 (2013).
51. J. Wüst, N. M. Sullivan, U. Hardegger, T. D. Wilkins, Investigation of an outbreak of antibiotic-associated colitis by various typing methods. *J. Clin. Microbiol.* **16**, 1096–1101 (1982).
52. M. Sebaihia, B. W. Wren, P. Mullany, N. F. Fairweather, N. Minton, R. Stabler, N. R. Thomson, A. P. Roberts, A. M. Cerdeño-Tárraga, H. Wang, M. T. Holden, A. Wright, C. Churcher, M. A. Quail, S. Baker, N. Bason, K. Brooks, T. Chillingworth, A. Cronin, P. Davis, L. Dowd, A. Fraser, T. Feltwell, Z. Hance, S. Holroyd, K. Jagels, S. Moule, K. Mungall, C. Price, E. Rabbinowitsch, S. Sharp, M. Simmonds, K. Stevens, L. Unwin, S. Whithead, B. Dupuy, G. Dougan, B. Barrell, J. Parkhill, The multidrug-resistant human pathogen *Clostridium difficile* has a highly mobile, mosaic genome. *Nat. Genet.* **38**, 779–786 (2006).
53. X. Chen, K. Katchar, J. D. Goldsmith, N. Nanthakumar, A. Cheknis, D. N. Gerding, C. P. Kelly, A mouse model of *Clostridium difficile*–associated disease. *Gastroenterology* **135**, 1984–1992 (2008).
54. S. W. Pawlowski, G. Calabrese, G. L. Kolling, J. Platts-Mills, R. Freire, C. AlcantaraWarren, B. Liu, R. B. Sartor, R. L. Guerrant, Murine model of *Clostridium difficile* infection with aged gnotobiotic C57BL/6 mice and a BI/NAP1 strain. *J. Infect. Dis.* **202**, 1708–1712 (2010).
55. W. N. Al-Nassir, A. K. Sethi, Y. Li, M. J. Pultz, M. M. Riggs, C. J. Donskey, Both oral metronidazole and oral vancomycin promote persistent overgrowth of vancomycin-resistant enterococci during treatment of *Clostridium difficile*-associated disease. *Antimicrob. Agents Chemother.* **52**, 2403–2406 (2008).
56. E. C. Oldfield IV, E. C. Oldfield III, D. A. Johnson, Clinical update for the diagnosis and treatment of *Clostridium difficile* infection. *World J. Gastrointest. Pharmacol. Ther.* **5**, 1–26 (2014).
57. T. J. Louie, M. A. Miller, K. M. Mullane, K. Weiss, A. Lentnek, Y. Golan, S. Gorbach, P. Sears, Y.-K. Shue; OPT-80-003 Clinical Study Group, Fidaxomicin versus vancomycin for *Clostridium difficile* infection. *N. Engl. J. Med.* **364**, 422–431 (2011).
58. I. Kreimeyer, F. Euler, A. Marckscheffel, H. Tatge, A. Pich, A. Olling, J. Schwarz, I. Just, R. Gerhard, Autoproteolytic cleavage mediates cytotoxicity of *Clostridium difficile* toxin A. *Naunyn Schmiedeberg's Arch. Pharmacol.* **383**, 253–262 (2011).
59. G. Yang, B. Zhou, J. Wang, X. He, X. Sun, W. Nie, S. Tzipori, H. Feng, Expression of recombinant *Clostridium difficile* toxin A and B in *Bacillus megaterium*. *BMC Microbiol.* **8**, 192 (2008).
60. S. Bagrodia, S. J. Taylor, C. L. Creasy, J. Chernoff, R. A. Cerione, Identification of a mouse $p21^{Cdc42/Rac}$ activated kinase. *J. Biol. Chem.* **270**, 22731–22737 (1995).
61. J. Tam, G. L. Beilhartz, A. Auger, P. Gupta, A. G. Therien, R. A. Melnyk, Small molecule inhibitors of *Clostridium difficile* toxin B-induced cellular damage. *Chem. Biol.* **22**, 175–185 (2015).
62. J. Inglese, D. S. Auld, A. Jadhav, R. L. Johnson, A. Simeonov, A. Yasgar, W. Zheng, C. P. Austin, Quantitative high-throughput screening: A titration-based approach that efficiently identifies biological activities in large chemical libraries. *Proc. Natl. Acad. Sci. U.S.A.* **103**, 11473–11478 (2006).
63. V. Brandes, I. Schelle, S. Brinkmann, F. Schulz, J. Schwarz, R. Gerhard, H. Genth, Protection from *Clostridium difficile* toxin B-catalysed Rac1/Cdc42 glucosylation by tauroursodeoxycholic acid-induced Rac1/Cdc42 phosphorylation. *Biol. Chem.* **393**, 77–84 (2012).
64. R. N. Pruitt, B. Chagot, M. Cover, W. J. Chazin, B. Spiller, D. B. Lacy, Structure-function analysis of inositol hexakisphosphate-induced autoprocessing in *Clostridium difficile* toxin A. *J. Biol. Chem.* **284**, 21934–21940 (2009).

Acknowledgments: We thank D. Mochly-Rosen, K. Grimes, and E. Egeler of the Stanford SPARK Translational Research Program for continued advice and support for the project. We thank the SPARK Advisory Board members, especially D. Erlanson (Carmot Therapeutics) and S. Schow (Telik Inc.), for general discussions and advice on the project direction. We are also grateful to R. Luong, Staff Pathologist and Senior Research Scientist at the Stanford Veterinary Service Center, and D. Imai, Pathologist and Clinical Professor at UC Davis, who provided pathology scoring for this research; J. Ballard of University of Oklahoma Health Sciences Center for advice on the mouse toxigenic model of CDI; H. Feng of the Department of Microbial Pathogenesis, University of Maryland Dental School, for the antibodies against GTD; and R. Melnyk and G. Beilhartz of the Department of Molecular Structure and Function, The Hospital for Sick Children, for reagents. **Funding:** This work was supported by a seed grant from the Stanford University SPARK Translational Research Program as well as by funding from the NIH R01-EB005011 (to M.B. with supplement for K.O.B.) and Stanford Innovation Project from Stanford Office of Technology Licensing. **Author contributions:** K.O.B. and M.G. designed, performed, and analyzed all experiments and drafted the paper. J.A.F. and A.J.H. developed a mouse model of CDI and performed *C. difficile* CFU counts. D.E.S.-C. performed the fluorescence polarization high-throughput screen and helped with the analysis of the screening results. M.A.C. assisted in biochemical aspects of the manuscripts and helped in design of in vitro experiments. S.K.H. and E.S. assisted with the animal work. A.W.P. synthesized TAMRA–AWP-19 probe, helped in the study design, and participated in the discussion of the project. A.S. constructed plasmids for toxin purification, purified toxins used in assays, optimized assays for measuring TAMRA–AWP-19 labeling, and helped develop the TAMRA–AWP-19 probe. N.B. provided and analyzed clinical samples from CDI patients. M.A.C., A.S., and J.L.S. evaluated experiments and edited the manuscript. M.B. developed and coordinated the project, evaluated the data, and prepared the manuscript. **Competing interests:** M.B., A.S., A.W.P., and K.O.B. are listed on a provisional patent WIPO Application Serial No. US2015/037242 entitled "Use of small molecules for the treatment of *Clostridium difficile* toxicity." The other authors declare that they have no competing interests.

Submitted 26 June 2015
Accepted 4 September 2015
Published 23 September 2015
10.1126/scitranslmed.aac9103

Citation: K. O. Bender, M. Garland, J. A. Ferreyra, A. J. Hryckowian, M. A. Child, A. W. Puri, D. E. Solow-Cordero, S. K. Higginbottom, E. Segal, N. Banaei, A. Shen, J. L. Sonnenburg, M. Bogyo, A small-molecule antivirulence agent for treating *Clostridium difficile* infection. *Sci. Transl. Med.* **7**, 306ra148 (2015).